THE JOURNAL OF PHYSICAL CHEMISTRY Letters

Letter

pubs.acs.org/JPCL

Free Energies of Cavity and Noncavity Hydrated Electrons Near the Instantaneous Air/Water Interface

Jennifer R. Casey,[†] Benjamin J. Schwartz,*[,†] and William J. Glover*[,‡,§,∥]

[†]Department of Chemistry and Biochemistry, University of California, Los Angeles, Los Angeles, California 90095-1569, United States

[‡]NYU-ECNU Center for Computational Chemistry, New York University Shanghai, Shanghai 200122, China

[§]Department of Chemistry, New York University, New York, New York 10003, United States

[∥]Department of Chemistry, East China Normal University, Shanghai 200062, China

Supporting Information

ABSTRACT: The properties of the hydrated electron at the air/water interface are computed for both a cavity and a noncavity model using mixed quantum/classical molecular dynamics simulation. We take advantage of our recently developed formalism for umbrella sampling with a restrained quantum expectation value to calculate free-energy profiles of the hydrated electron's position relative to the water surface. We show that it is critical to use an instantaneous description of the air/water interface rather than the Gibbs' dividing surface to obtain accurate potentials of mean force. We find that noncavity electrons, which prefer to encompass several water molecules, avoid the interface where water molecules are scarce. In contrast, cavity models of the hydrated electron, which prefer to expel water, have a local free-energy minimum near the interface. When the cavity electron occupies this minimum, its absorption spectrum is quite red-shifted, its binding energy is significantly lowered, and its dynamics speed up quite a bit compared with the bulk, features that have not been found by experiment. The surface activity of the electron therefore serves as a useful test of cavity versus noncavity electron solvation.

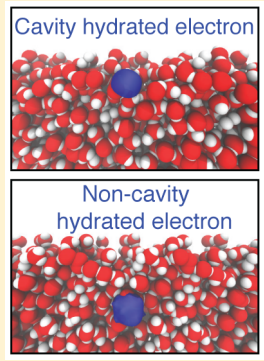

In recent years, the structure of the hydrated electron, which is perhaps the simplest possible quantum mechanical solute, has been the center of much debate.[1−10] Despite intense experimental and theoretical investigation, it is still unclear whether the structure of an excess electron in liquid water is best thought of as something similar to a halide ion, where most of the electron resides in a solvent cavity,[11] as an "inverse plum pudding" or "noncavity" electron, where water molecules are packed within the electron's wave function (possibly even to a higher density than in bulk liquid water),[1,7] or as a hybrid of these two pictures, with strong overlap between the electron's wave function and the first-shell water molecules that surround a small central cavity.[8,12] However, as of yet, no single model captures all of the subtle details of the hydrated electron that are known from experiment; for example, our noncavity model predicts resonance Raman spectra and the temperature dependence of the absorption spectrum in accord with experiment, features that are not properly accounted for by cavity models,[6] but, as discussed further below, our noncavity model also predicts a large negative molar volume of solvation for the hydrated electron, in contrast with both cavity models and experiment.[13,14]

In addition to the studies on the structure of the bulk hydrated electron, there has also been recent interest in the nature of hydrated electrons at the air/water interface. Over the past few years, experimentalists have developed the ability to perform photoelectron spectroscopy (PES) on excess electrons in liquid water microjets under high vacuum.[9,10,15−18] This raises the possibility of using the surface activity of the hydrated electron as an additional experimental observable to test the predictions of cavity and noncavity models. In particular, cavity models predict that hydrated electrons behave like quasi-spherical polarizable ions with a diameter roughly comparable to bromide,[19] so one might expect cavity hydrated electrons to prefer to reside at the interface, similar to the larger halides.[20] Conversely, one might expect that noncavity hydrated electrons, which prefer to encompass water packed at high densities, would favor bulk solvation because the density of water decreases near the interface.

In pioneering microjet studies on the PES of the hydrated electron, Abel et al. observed two different distinct vertical binding energies (VBEs) for the hydrated electron: one at ∼3.3 eV, which was assigned to the bulk value, and a second at ∼1.6 eV, roughly half of the bulk value, which was assigned to a hydrated electron localized at the air/water interface.[9] However, several subsequent vacuum microjet PES studies re-examined the hydrated electron system and instead found only a single peak assigned to the bulk VBE value at ∼3.6 eV.[10,15−17] To make matters even more potentially confusing, recent theoretical results have suggested that interfacial hydrated

Received: May 26, 2016
Accepted: August 1, 2016

DOI: 10.1021/acs.jpclett.6b01150
J. Phys. Chem. Lett. 2016, 7, 3192−3198

electrons may still have a complete first solvation shell, giving them essentially identical energetics to those of the bulk.[21]

The behavior of interfacial hydrated electrons also has been explored experimentally by second harmonic generation (SHG), a surface-specific nonlinear optical spectroscopy.[22] Verlet and coworkers were able to observe a time-dependent SHG signal originating from hydrated electrons, but the kinetics of the observed signal matched that of bulk hydrated electrons.[22] Furthermore, these authors were only able to determine that the hydrated electrons resided <1 nm from the interface. Because 1 nm is roughly three water molecular diameters, this means that the SHG experiment could effectively be probing hydrated electrons in the bulk.[22−24] It is also worth noting that pulse-radiolysis experiments that produced hydrated electrons in water that was confined in 1 nm diameter silica pore glasses found that the confined electrons retain their bulk absorption spectrum, consistent with the idea that electrons need to be closer than 0.5 nm to a surface if non-bulk-like interfacial properties are to be detected.[25]

The purpose of this Letter is therefore 3-fold: (1) to explore, by mixed quantum/classical molecular dynamics (MQC MD) simulation, the surface activity of the hydrated electron as a further test of cavity versus noncavity models; (2) to predict how the vertical binding energy of the hydrated electron changes near an air/water interface and to compare these predictions to PES experiments; and (3) to discover how the properties of different models of the hydrated electron vary as a function of distance from the interface, in an attempt to reconcile the nonlinear optical and PES experimental findings.

To address these goals, we turn to a recent methodological development from our group that enables calculation of free energies for quantum mechanical objects,[24] which we refer to as the "quantum-biased molecular dynamics" method (QBMD). Our method is based on applying traditional classical umbrella sampling to a coordinate that involves an expectation value of a quantum mechanical object in a mixed quantum/classical simulation. For the problem at hand, the relevant quantity is the vertical distance of the expectation value of the electron's position from the air/water interface. We previously demonstrated the use of QBMD to calculate the free energy of a cavity-hydrated electron relative to the Gibbs' dividing surface (GDS) of the air/water interface.[24] Although the GDS is simple to compute, it ignores the molecular details of the fluctuating liquid surface that can cause large changes in the calculated potentials of mean force (PMFs) of ions at the air/water interface.[26] Thus, in this work, we extend the QBMD method to calculate PMFs of both cavity and noncavity hydrated electron models relative to the *instantaneous* air/water interface.[27] As we show below in the Computational Methods section, the classical forces needed to restrain the electron in this case are nontrivial as both the location of the instantaneous interface and the electron's center of mass simultaneously depend on the positions of all of the water molecules in the simulation.

In mixed quantum/classical simulations, the structure of the hydrated electron is determined by the pseudopotential chosen to represent the interactions between the quantum mechanical electron and the classical water molecules. However, relatively small differences between pseudopotentials can lead to entirely different predicted hydrated electron structures. For example, both the cavity potential developed by Turi and Borgis[28] (TB) and the noncavity potential developed previously in our group (denoted LGS in the literature)[1] were derived from the Phillips−Kleinman pseudopotential formalism; the only difference between them is the fitting function chosen to represent the numerically determined potential.[7]

We thus begin by examining the PMFs for both the TB cavity and LGS noncavity electrons relative to the instantaneous interface, calculated from our QBMD method, which are shown in Figure 1. It is clear that the LGS noncavity electron is

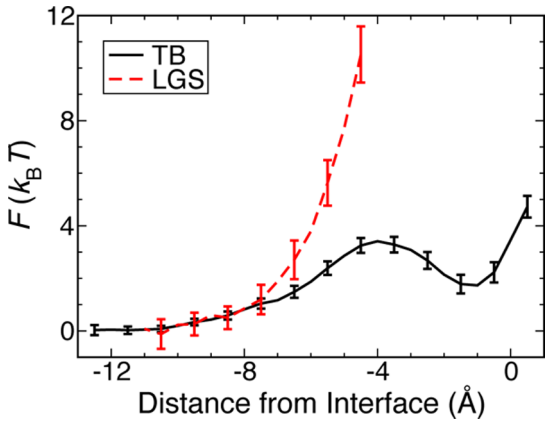

Figure 1. PMF (i.e., Helmholtz free energy) for cavity TB (black solid curve) and noncavity LGS (red dashed curve) hydrated electrons as a function of vertical distance from the instantaneous air/water interface. Negative distances indicate displacements below the instantaneous interface. It is clear that the LGS noncavity electron avoids the interface, with a substantial free-energy penalty for approaching within 0.5 nm of the surface. The TB cavity electron, in contrast, shows only a small energetic penalty (~1.5 k_BT) for interfacial solvation, with a local minimum only ~1 Å below the interface. The error bars reflect the statistical uncertainty from 80-ps trajectories for the LGS electron and 200-ps trajectories for the TB electron in each umbrella window.

strongly repelled by the air/water interface (red dashed curve) and favors solvation away (>9 Å) from the interface. Bringing the electron even one water diameter closer to the interface at 6 Å destabilizes the system by ~4 k_BT, and a system in which the electron lies just another 1 Å closer, or 0.5 nm from the interface, is destabilized by ~10 k_BT. Indeed, we were unable to restrain the LGS electron closer than 4.5 Å from the interface without the biasing forces being so large as to cause numerical instability. This result is perhaps not all that surprising. The LGS electron is a highly hydrophilic object that prefers, on average, to encompass regions of high water density.[1] Thus, the reduced water density near the interface is incompatible with the LGS electron's noncavity structure, to the point where a thermally equilibrated LGS electron will simply not approach within ~6 Å of an air/water interface.

In contrast, the TB cavity electron (black solid curve) exhibits a local minimum in its PMF at only ~1 Å below the instantaneous interface; this minimum lies only ~1.5 k_BT above that of the PMF minimum at ~12 Å and can be reached by fluctuations over a modest ~3 k_BT barrier. This is similar to the barrier seen in the interfacial activity of the halide ions[26] and likely has the same origin: an inability of surface water molecules to simultaneously solvate the ion in the barrier region while maintaining their preferred orientation of having one O−H bond pointing into the vapor phase and one O−H bond available for hydrogen bonding within the layer.[26,27] Overall, the TB cavity model predicts that there should be a measurable population of electrons that reside at (i.e., within ~4 Å of) the air/water interface.

DOI: 10.1021/acs.jpclett.6b01150
J. Phys. Chem. Lett. 2016, 7, 3192−3198

It is important to note that the PMF for the TB electron relative to the instantaneous air/water interface looks quite different from that in our previous work where the GDS was used to characterize the interface (compare Figure 1 this Letter and Figure 4a in ref 24). When the GDS is used, instantaneous fluctuations in the height of the interface smear out the barrier, leaving only a free-energy plateau below the interface. The free-energy features we see in the PMF using the instantaneous interface, however, are more consistent with previously performed MD trajectories of the TB electron, which found that at low temperatures the TB electron persists in the interfacial region for >100 ps, and under ambient conditions for ~10 ps,[23] presumably the result of being trapped in the local free-energy minimum. Thus, it is clear that the use of the instantaneous interface is critical to providing a proper free-energy picture of the interfacial solvation of hydrated electrons.

How does the hydrated electron free-energy picture painted in Figure 1 stack up against the various interfacial experiments? We begin by considering the photoelectron spectrum, which in the Condon approximation is trivial to calculate from the simulated trajectories by finding the distribution of energy differences between neutral and anionic systems with the nuclei fixed at each MD snapshot (see SI for more details). It is worth noting that the absolute binding energies we predict for the LGS electron are too high relative to experiment, as is now well-documented for this model.[1−4] Rather than attempt to correct this deficiency, which would entail developing a new pseudopotential, an exercise that is beyond the scope of this Letter, we instead focus instead on relative changes in the binding energy of the electron as a function of distance from the air/water interface.

Figure 2a shows the predicted photoelectron spectrum for the LGS noncavity electron at distances >9 Å below the surface (black solid curve) and at a distance of 6 ± 0.2 Å below the surface (green dashed curve); as mentioned above, we were unable to restrain the LGS electron to lie closer than 4.5 Å below the interface. The photoelectron spectrum at >9 Å agrees with the bulk VBE of the LGS model,[1,3,5] which, taken together with the repulsive nature of the PMF in Figure 1, indicates that the LGS electron shows only bulk-like behavior, consistent with the majority of the recent PES experiments.[10,15−18] Interestingly, the predicted photoelectron spectrum at 6 Å is also indistinguishable from the bulk VBE (within error), suggesting that bulk-like solvation is attained at a depth of only two water diameters from the instantaneous interface, further reinforcing our conclusion that the LGS electron shows only bulk-like behavior.

On the other hand, because the free-energy profile has a local minimum near the instantaneous air/water interface, the story for the TB cavity hydrated electron is quite different. In particular, the PMF that we compute predicts that in a pump−probe experiment electrons generated at the interface will be quasi-stable and, due to the free energy barrier, will persist there for some time before diffusing to the bulk. Indeed, as mentioned above, previous simulations with the TB model under ambient conditions found a time scale of ~10 ps for this process.[23] The question thus becomes whether such kinetically stable TB interfacial electrons can be distinguished from those in the bulk. Figure 2b shows the predicted thermally averaged photoelectron spectrum of the TB electron in the interfacial region (<4 Å below the surface, blue dotted curve), bulk region (>9 Å below the interface, black solid curve), and at 6 ± 0.2 Å (dashed green curve). We see that interfacial solvation reduces

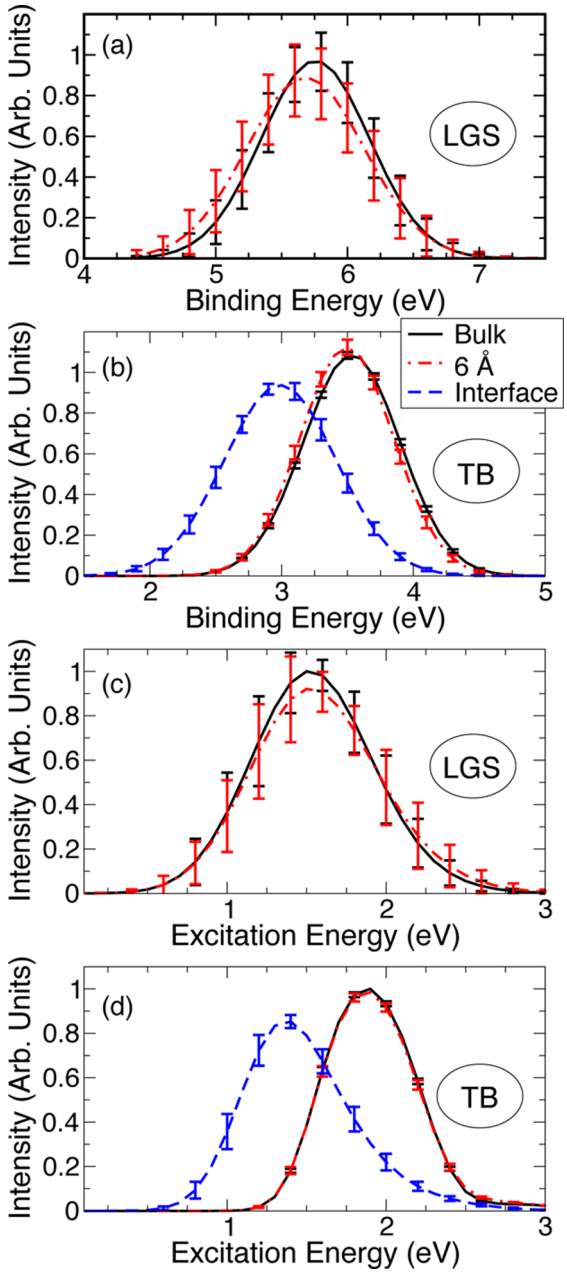

Figure 2. Spectroscopic properties of the interfacial hydrated electron. Thermally averaged calculated photoelectron spectra of (a) TB cavity and (b) LGS noncavity hydrated electrons. Panels c and d show the different hydrated electron models' thermally averaged optical absorption spectra for varying distances from the instantaneous air−water interface. For all panels, properties are shown at the interface (<4 Å, dashed blue curve, TB only), near the interface (6 ± 0.2 Å, dotted-dashed red curves), and in the bulk (distances >9 Å, solid black curve). Clearly, the LGS electron displays only bulk-like behavior at all thermally accessible distances, while the interfacial TB electron has a significantly reduced electron binding energy and red-shifted absorption spectrum. However, the effect of the interface is short-ranged, and both models exhibit bulk-like properties at distances ≥6 Å below the interface.

the TB electron's VBE by ~0.5 eV relative to the bulk, which should be experimentally identifiable. This signature, however, has been seen in neither steady-state PES experiments[10] nor in more recent time-resolved PES experiments[15,17,18] (except possibly in the experiments of Abel and coworkers,[9] mentioned

DOI: 10.1021/acs.jpclett.6b01150
J. Phys. Chem. Lett. 2016, 7, 3192−3198

above). The lack of signal identifiable to a surface electron in the time-resolved PES studies is significant because these experiments generated hydrated electrons by photodetachment from aqueous iodide, which is a surface-active anion.[26] One would thus expect a surface excess of hydrated electrons at early pump−probe time delays, but instead, these studies found evidence only for bulk solvation following an ultrafast (∼1 ps) relaxation time scale.

We note that our finding that the VBE of the TB electron decreases at the interface is also at odds with recent QM/MM simulations that predict that interfacial electrons have a binding energy that is essentially unchanged from the bulk.[21] It is possible, however, that the DFT-based description or the lack of polarization and dispersion interactions between the QM and MM systems in this QM/MM work leads to an imbalanced description of the binding energy at the interface and bulk, and further exploration is needed. It is clear, however, that the effects of the interface are short-ranged and that both the TB and LGS electron at 6 Å or more below the interface have essentially bulk properties.

In addition to the photoelectron spectrum, we also investigated the optical absorption spectrum of the different models of the hydrated electron at the air/water interface. We find in Figure 2c that the absorption spectrum of LGS for distances >9 Å from the interface (solid black curve) is slightly red-shifted from the bulk absorption spectrum of this model computed with cutoff electrostatics.[1] However, this red shift is consistent with what Herbert and coworkers found when Ewald summation is used to handle electrostatics;[5] therefore, the spectrum at these distances corresponds to the bulk predictions of this model. Similar to the behavior of the VBE, we find in Figure 2c that the absorption spectrum of the LGS noncavity electron at 6 Å from the interface (dashed green curve) matches the bulk spectrum (within error), a result consistent with the observation that hydrated electrons confined within ∼1 nm diameter silica nanopores also retain bulk-like spectral properties.[25] Like LGS, the TB cavity electron at 6 Å from the air/water interface also has an absorption spectrum indistinguishable from the bulk (Figure 2d, dashed green and solid black curves, respectively); however, the absorption spectrum in the PMF minimum at the interface (dotted blue curve) is noticeably red-shifted. This spectral shift is a direct reflection of the fact that the TB electron's radius of gyration increases from ∼2.2 Å in the bulk to ∼3 Å near the interface; the magnitude of the electron's size fluctuations also increases as the electron moves toward the interface. In combination with the lowered VBE, this is a clear indication that the TB cavity electron becomes partially desolvated at the interface.

The partial desolvation and lower density and viscosity of water at the interface also result in changes in the dynamics of the water molecules surrounding the interfacial TB electron. As an example of solvent kinetics, Figure 3 plots the diffusion constant of the TB cavity electron (in the plane parallel to the GDS) as a function of distance of the electron's center-of-mass from the instantaneous interface. As might be expected, the diffusion constant of the TB electron is significantly higher when localized in the PMF minimum at the interface than in the bulk.

The fact that the TB cavity electron can reside at the interface (and shows different spectroscopy and kinetics while at the interface) but the LGS noncavity electron shows only bulk behavior can be compared with the SHG experiment performed by Verlet and coworkers.[22] These experiments

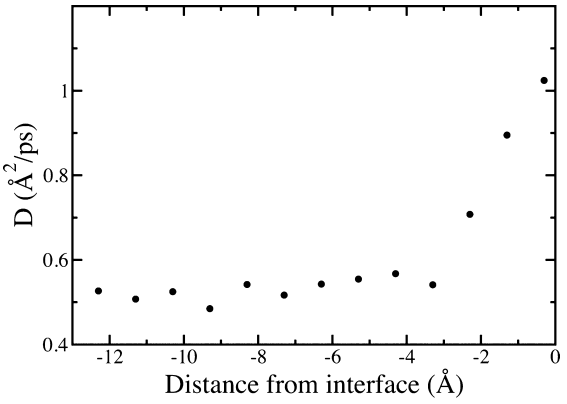

Figure 3. Diffusion constant of the TB cavity electron in the plane parallel to the (GDS) interface as a function of distance of the electron's center of mass away from the interface (data for LGS not shown because the LGS electron diffusion constant does not change over any thermally accessible distance from the interface). The speed-up of the TB electron's dynamics near the interface is expected due to the lower density and viscosity of water in this region.

showed that the kinetics of hydrated electrons seen by SHG were identical to those in the bulk, consistent with the LGS model but not with the presence of an interfacial cavity electron. In particular, because Verlet and coworkers provided an upper bound of 1 nm on the depth of SHG-active electrons,[22] we interpret the SHG signal in these experiments as arising only from hydrated electrons residing at least ∼0.6 nm below the surface rather than at the interface, making these experiments more consistent with the features of the PMF of the LGS noncavity model.

In summary, we have simulated the properties and free energies of both a cavity and a noncavity model of the hydrated electron as a function of distance from the instantaneous air/water interface. Our main conclusion is that the surface activity of the electron is a useful observable that distinguishes cavity from noncavity models of the electron. In particular, we find that the LGS noncavity electron prefers to avoid the interface, with a significant free-energy penalty to drag the electron within 5 Å of the instantaneous surface. In contrast, the TB cavity electron has a local free-energy minimum at the interface that is only slightly higher than that for the electron to reside in the bulk. The free-energy minimum does not exist when the interface is described by the Gibbs' dividing surface, highlighting the importance of using an instantaneous description of the interface in this type of calculation. When the TB cavity electron resides near the interface, we find that its binding energy is significantly lowered compared with the bulk, a property that (so far) has not been found by PES experiments, with the possible exception of one study by Abel and coworkers.[9] However, our simulations predict that bulk-like properties will be seen for both cavity and noncavity models at distances larger than 6 Å below the surface (about two solvent shells), indicating that care must be taken in spectroscopic experiments to separate signals arising from bulk and interfacial hydrated electrons.

After submission of our manuscript, a new study by Tahara and coworkers was published that explored the influence of hydrated electrons on the sum frequency generation (SFG) spectra of interfacial water.[29] Their analysis gave a picture of partially solvated interfacial electrons that decay into the bulk on a ∼10 ps time scale, a finding that would seem to be more

DOI: 10.1021/acs.jpclett.6b01150
J. Phys. Chem. Lett. 2016, 7, 3192−3198

consistent with the predictions of the TB cavity model than the LGS noncavity model. It is clear that further work is needed to reconcile the findings of PES, SHG, and SFG experiments on the hydrated electron. In particular, a better understanding of and control over the probing depth of PES, time-resolved PES, and nonlinear optical experiments is needed, together with more information on the initial distribution of interfacial depths of hydrated electrons produced following ionization of a surface-active solute.

Although a determination of cavity or noncavity structure from the experimental interfacial properties of the hydrated electron is currently inconclusive, we believe that, taking the body of experimental evidence on all of the known properties of the hydrated electron, noncavity models are still favored. In particular, although cavity and noncavity models do about equally well in predicting the absorption spectrum/radius of gyration and pump−probe transient absorption spectroscopy of the hydrated electron,[1] the noncavity model does significantly better at explaining the temperature dependence of the electronic absorption spectrum and the resonance Raman spectrum of the hydrated electron.[6] However, as discussed below, the LGS noncavity model predicts a molar solvation volume that is simply too negative to be consistent with experiment. We believe that the noncavity picture of the hydrated electron is basically correct but that the LGS model is somewhat overattractive, as evidenced by its VBE overprediction and thus places too much water density in the electron's interior. Hopefully future work will converge on a model that is consistent with all the known properties of the hydrated electron, and we believe that such a model will have a significant number of water molecules residing in the electron's interior.

COMPUTATIONAL METHODS

Our simulations of the hydrated electrons followed the same protocols we developed and used in previous work.[6,7,24] In brief, the system consisted of one quantum-mechanical electron that interacted with 499 flexible simple point charge (SPC-Flex) water molecules[30] using either the TB cavity[28] or LGS noncavity[1] pseudopotentials. To simulate the air/water interface, the x- and y-axis lengths of the simulation box were fixed at L = 24.64 Å, while the z axis was extended to $5L$. The quantum-mechanical wave function was represented on a Fourier grid, whose length was altered to account for the increased size of the electron at the interface. We found that for the LGS electron, a 32 × 32 × 32 grid basis set with a spacing of 0.56 Å between grid points was sufficient to converge the quantum energy to better than 0.01 eV. For the TB electron, we used a grid basis of size 14 × 14 × 14 for umbrella windows centered between 12.5 and 2.5 Å below the interface, 18 × 18 × 18 for windows between 2 and 0.5 Å below the interface, and 22 × 22 × 22 for the window centered at 0.0 Å below the interface to achieve the same level of convergence; in all trajectories using the TB potential the grid spacing was 1.12 Å. Periodic boundary conditions were applied in all directions, and electrostatic interactions were calculated using 3-D Ewald summation (EW3D), with $z = 5L$.[31,32] The quantum adiabatic eigenstates were found at every time step using the Davidson algorithm,[33] and the quantum forces on the classical particles were evaluated using the Hellmann−Feynman Theorem.[34] Dynamics was propagated using the Velocity Verlet algorithm with a 1.0 fs time step,[35] and the canonical (NVT) ensemble was sampled at 298 K with Bussi's stochastic thermostat.[36]

To calculate distances from the interface, instead of using the Gibbs' dividing surface, we utilized the instantaneous, atomistic description of the air/water interface developed by Willard and Chandler[27] and refined by Varrily and Chandler.[37] We refer the reader to the Supporting Information for details, but in brief, the instantaneous interface is defined as the isosurface above a water slab where a coarse-grained density field, $\phi(\mathbf{r})$, decays to half of the bulk density. To construct the potentials of mean force relative to the instantaneous interface, we ran a series of MQC MD trajectories using our recently developed quantum expectation value umbrella sampling method, QBMD.[24] Further details, including the chain rules needed to calculate the biasing forces for restraining the expectation value of the electron's position relative to the instantaneous interface, are provided in the Supporting Information.

Finally, although the interfacial simulations were run in the canonical (NVT) ensemble, in the interfacial simulations, the water slab occupies only ∼20% of the total available volume. This means that in essence the water slab in these simulations is held at a fixed pressure. This makes it possible to estimate the molar solvation volume of the TB cavity and LGS noncavity hydrated electrons by comparing the volume of the water slab in trajectories with and without the addition of the quantum electron. To calculate the partial molar volume of the electron, we used unbiased simulations of 50 ps and represented the interfaces on a grid of 100 × 100, with a grid spacing of 0.243 Å. We found a molar solvation volume of +31 ± 12 cm^3/mol and −116 ± 27 cm^3/mol for the TB and LGS electrons, respectively. These values agree with our intuition: cavity-hydrated electrons exclude water, resulting in an increased volume of the water + electron slab, while the LGS electron packs interior waters to higher density, decreasing the overall volume of the slab.

When comparing these molar solvation numbers to experiment, it should be noted that there is some discrepancy as to what the experimental molar solvation volume of the hydrated electron actually should be. The experiments that measure this quantity involve shifts in the equilibrium of some chemical reaction that involves the hydrated electron, where the solvation volume changes of the other reactants are known or at least can be estimated. We are aware of two experiments aimed at obtaining the molar solvation volume of the hydrated electron: a pulse radiolysis experiment at high pressures that gave a partial molar volume of −5.9 cm^3/mol,[13] and a time-resolved photoacoustic study that gave a value of +26 cm^3/mol.[14] The calculated TB cavity electron's partial molar volume agrees well with the photoacoustic experimental results, while the LGS noncavity electron's partial molar volume has the same sign as the radiolysis experiments but a magnitude that is much greater. The fact that the LGS electron has such a high density of water in its interior is likely unphysical. This fits with our previous work, showing that the LGS electron overestimates the shift of the temperature-dependent optical absorption spectrum by a factor of ∼2.5 due to its overly attractive nature.[6] In future work, we will show that the water density in the interior of the LGS noncavity electron is highly temperature-dependent, so it is possible that the scale of attraction of the LGS pseudopotential is simply too large relative to the temperatures being simulated but that there is still a significant amount of water in the electron's interior.

DOI: 10.1021/acs.jpclett.6b01150
J. Phys. Chem. Lett. 2016, 7, 3192−3198

■ ASSOCIATED CONTENT

Supporting Information

The Supporting Information is available free of charge on the ACS Publications website at DOI: 10.1021/acs.jpclett.6b01150.

Detailed description of how our quantum-biased molecular dynamics method was extended to handle an instantaneous air/water interface to generate the potentials of mean force in Figure 1. We then provide a verification of our simulation protocol on the PMF of (classical) aqueous iodide relative to the instantaneous air/water interface. Finally, we include a description of how we generated photoelectron spectra and optical absorption spectra of the hydrated electron as a function of distance from the instantaneous air/water interface. (PDF)

■ AUTHOR INFORMATION

Corresponding Authors

*B.J.S.: E-mail: schwartz@chem.ucla.edu.
*W.J.G.: E-mail: william.glover@nyu.edu.

Notes

The authors declare no competing financial interest.

■ ACKNOWLEDGMENTS

This work was supported by NSF grants CHE-1212951 and CHE-1565434 and ACS-PRF grant 55534-ND6. Computational resources were provided by the UCLA Institute for Digital Research and Education and the California NanoSystems Institute. W.J.G. thanks NYU Shanghai for start-up funds and the NYU Shanghai High Performance Computing Center for hosting his computing resources.

■ REFERENCES

(1) Larsen, R. E.; Glover, W. J.; Schwartz, B. J. Does the hydrated electron occupy a cavity? *Science* **2010**, *329*, 65−69.
(2) Turi, L.; Madarasz, A. Comment on "Does the hydrated electron occupy a cavity? *Science* **2011**, *331*, 1387c.
(3) Jacobson, L. D.; Herbert, J. M. Comment on "Does the hydrated electron occupy a cavity? *Science* **2011**, *331*, 1387−d.
(4) Larsen, R. E.; Glover, W. J.; Schwartz, B. J. Response to comments on "Does the hydrated electron occupy a cavity? *Science* **2011**, *331*, 1387e.
(5) Herbert, J. M.; Jacobson, L. D. Structure of the aqueous electron: Assessment of one-electron pseudopotential models in comparison to experimental data and time-dependent density functional theory. *J. Phys. Chem. A* **2011**, *115*, 14470−14483.
(6) Casey, J. R.; Larsen, R. E.; Schwartz, B. J. Resonance Raman and temperature-dependent electronic absorption spectra of cavity and noncavity models of the hydrated electron. *Proc. Natl. Acad. Sci. U. S. A.* **2013**, *110*, 2712−2717.
(7) Casey, J. R.; Kahros, A.; Schwartz, B. J. To be or not to be in a cavity? The hydrated electron dilemma. *J. Phys. Chem. B* **2013**, *117*, 14173−14182.
(8) Uhlig, F.; Marsalek, O.; Jungwirth, P. Unraveling the complex nature of the hydrated electron. *J. Phys. Chem. Lett.* **2012**, *3*, 3071−3075.
(9) Siefermann, K. R.; Liu, Y.; Lugovoy, E.; Link, O.; Faubel, M.; Buck, U.; Winter, B.; Abel, B. Binding energies, lifetimes and implications of bulk and interface solvated electrons in water. *Nat. Chem.* **2010**, *2*, 274−279.
(10) Shreve, A. T.; Yen, T. A.; Neumark, D. M. Photoelectron spectroscopy of hydrated electrons. *Chem. Phys. Lett.* **2010**, *493*, 216−219.
(11) Kevan, L. Solvated electron structure in glassy matrices. *Acc. Chem. Res.* **1981**, *14*, 138−145.
(12) Kumar, A.; Walker, J. A.; Bartels, D. M.; Sevilla, M. D. A simple ab initio model for the hydrated electron that matches experiment. *J. Phys. Chem. A* **2015**, *119*, 9148−9159.
(13) Hentz, R. R.; Brazier, D. W. Radiolysis of liquids at high pressures. X. The reaction H + OH- and the partial molal volume of the hydrated electron. *J. Chem. Phys.* **1971**, *54*, 2777−2780.
(14) Borsarelli, C. D.; Bertolotti, S. G.; Previtali, C. M. Thermodynamic changes associated with the formation of the hydrated electron after photoionization of inorganic anions: a time-resolved photoacoustic study. *Photochem. Photobiol. Sci.* **2003**, *2*, 791−795.
(15) Lubcke, A.; Buchner, F.; Heine, N.; Hertel, I.; Schultz, T. Time-resolved spectroscopy of solvated electrons in aqueous NaI solutions. *Phys. Chem. Chem. Phys.* **2010**, *12*, 14629−14634.
(16) Tang, Y.; Shen, H.; Sekiguchi, K.; Kurahashi, N.; Mizuno, T.; Suzuki, Y.-I.; Suzuki, T. Direct measurement of vertical binding energy of a hydrated electron. *Phys. Chem. Chem. Phys.* **2010**, *12*, 3653−3655.
(17) Buchner, F.; Schultz, T.; Lubcke, A. Solvated electrons at the water-air interface: surface versus bulk signal in low kinetic energy photoelectron spectroscopy. *Phys. Chem. Chem. Phys.* **2012**, *14*, 5837−5842.
(18) Yamamoto, Y.-I.; Suzuki, Y.-I.; Tomasello, G.; Horio, T.; Karashima, S.; Mitríc, R.; Suzuki, T. Time- and angle-resolved photoemission spectroscopy of hydrated electrons near a liquid water surface. *Phys. Rev. Lett.* **2014**, *112*, 187603.
(19) Turi, L.; Borgis, D. Analytical investigations of an electron-water molecule pseudopotential. 2. Development of a new pair potential and molecular dynamics simulations. *J. Chem. Phys.* **2002**, *117*, 6186−6195.
(20) Tobias, D. J.; Stern, A. C.; Baer, M. D.; Levin, Y.; Mundy, C. J. Simulation and theory of ions at atmospherically relevant aqueous liquid-air interfaces. *Annu. Rev. Phys. Chem.* **2013**, *64*, 339−359.
(21) Uhlig, F.; Marsalek, O.; Jungwirth, P. Electron at the surface of water: Dehydrated or not? *J. Phys. Chem. Lett.* **2013**, *4*, 338−343.
(22) Sagar, D. M.; Bain, C. D.; Verlet, J. R. R. Hydrated electrons at the air/water interface. *J. Am. Chem. Soc.* **2010**, *132*, 6917.
(23) Madarasz, A.; Rossky, P. J.; Turi, L. Excess electron relaxation dynamics at water/air interfaces. *J. Chem. Phys.* **2007**, *126*, 234707.
(24) Glover, W. J.; Casey, J. R.; Schwartz, B. J. Free energies of quantum particles: The coupled-perturbed quantum umbrella sampling method. *J. Chem. Theory Comput.* **2014**, *10*, 4661−4671.
(25) Musat, R. M.; Cook, A. R.; Renault, J.-P.; Crowell, R. A. Nanosecond pulse radiolysis of nanoconfined water. *J. Phys. Chem. C* **2012**, *116*, 13104−13110.
(26) Stern, A. C.; Baer, M. D.; Mundy, C. J.; Tobias, D. J. Thermodynamics of iodide adsorption at the instantaneous air-water interface. *J. Chem. Phys.* **2013**, *138*, 114709.
(27) Willard, A. P.; Chandler, D. Instantaneous liquid interfaces. *J. Phys. Chem. B* **2010**, *114*, 1954−1958.
(28) Turi, L.; Gaigeot, M.-P.; Levy, N.; Borgis, D. Analytical investigations of an electron-water pseudopotential. 1. Exact calculation on a model. *J. Chem. Phys.* **2001**, *114*, 7805−7815.
(29) Matsuzaki, K.; Kusaka, R.; Nihonyanagi, S.; Yamaguchi, S.; Nagata, T.; Tahara, T. Partially hydrated electrons at the air/water interface observed by UV-excited time-resolved heterodyne-detected vibrational sum frequency generation spectroscopy. *J. Am. Chem. Soc.* **2016**, *138*, 7551−7557.
(30) Toukan, K.; Rahman, A. Molecular-dynamics study of atomic motions in water. *Phys. Rev. B: Condens. Matter Mater. Phys.* **1985**, *31*, 2643−2648.
(31) Spohr, E. Effect of electrostatic boundary conditions and system size on the interfacial properties of water and aqueous solutions. *J. Chem. Phys.* **1997**, *107*, 6342−6348.
(32) Ballenegger, V.; Arnold, A.; Cerda, J. J. Simulations of non-neutral slab systems with long-range electrostatic interactions in two-dimensional periodic boundary conditions. *J. Chem. Phys.* **2009**, *131*, 94107.

DOI: 10.1021/acs.jpclett.6b01150
J. Phys. Chem. Lett. 2016, 7, 3192−3198

(33) Davidson, E. R. The iterative calculation of a few of the lowest eigenvalues and corresponding eigenvectors of large real-symmetric matrices. *J. Comput. Phys.* **1975**, *17*, 87−94.
(34) Feynman, R. P. Forces in molecules. *Phys. Rev.* **1939**, *56*, 340.
(35) Verlet, L. Computer experiments on classical fluids I. Thermodynaical properties of Lennard-Jones molecules. *Phys. Rev.* **1967**, *159*, 98.
(36) Bussi, G.; Donadio, D.; Parrinello, M. Canonical sampling through velocity rescaling. *J. Chem. Phys.* **2007**, *126*, 014101.
(37) Varilly, P.; Chandler, D. Water evaporation: A transition path sampling study. *J. Phys. Chem. B* **2013**, *117*, 1419−1428.

DOI: 10.1021/acs.jpclett.6b01150
J. Phys. Chem. Lett. 2016, 7, 3192−3198